Thermodynamics of O(N) antiferromagnets in 2+1 dimensions

Christoph P. Hofmann
Facultad de Ciencias, Universidad de Colima, Bernal Díaz del Castillo 340, Colima CP 28045, Mexico
(Received 8 October 2009; revised manuscript received 14 December 2009; published 22 January 2010)

Within the framework of effective Lagrangians we calculate the free energy density for an O(N) antiferromagnet in 2+1 dimensions up to three-loop order in the perturbative expansion and derive the low-temperature series for various thermodynamic quantities. In particular, we show that the magnon-magnon interaction in the O(3) antiferromagnet in $d=2+1$—the O(3)-invariant quantum Heisenberg antiferromagnet on a square or a honeycomb lattice—is very weak and repulsive and manifests itself through a term proportional to five powers of the temperature in the free energy density. Remarkably, the corresponding coefficient is fully determined by the leading-order effective Lagrangian $\mathcal{L}^2_{eff}$ and does not involve any higher-order effective constants from $\mathcal{L}^4_{eff}$ related to the anisotropies of the lattice—the symmetries are thus very restrictive in $d=2+1$. We also compare our results that apply to O(N) antiferromagnets in 2+1 dimensions with those for O(N) antiferromagnets in 3+1 dimensions. The present work demonstrates the efficiency of the fully systematic effective Lagrangian method in the condensed-matter domain, which clearly proves to be superior to spin-wave theory. We would like to emphasize that the structure of the low-temperature series derived in the present work is model independent and universal as it only relies on symmetry considerations.

DOI: 10.1103/PhysRevB.81.014416 PACS number(s): 75.50.Ee, 75.30.Ds, 12.39.Fe, 11.10.Wx

I. INTRODUCTION

With the present paper we would like to further promote the effective Lagrangian method in the condensed-matter domain—in particular, we would like to demonstrate its efficiency in describing the thermodynamic properties of systems exhibiting collective magnetic behavior. While the low-energy properties of antiferromagnets in dimension $d=3+1$ have previously been investigated within the effective Lagrangian framework,[1–4] in the present study we focus our attention on antiferromagnets in dimension $d=2+1$. A thorough analysis of these condensed-matter systems, using effective-field theory methods, was performed in Refs. 1 and 5–8. However, in the present paper, we go one step further in the perturbative expansion, taking into account contributions to the free energy density up to three-loop order. The improvement by going from two- to three-loop order, as we will see, is that the interaction among the spin-wave degrees of freedom only starts manifesting itself at the three-loop level. Our new result that the magnon-magnon interaction in the O(3)-invariant quantum Heisenberg antiferromagnet on a square or a honeycomb lattice is very weak and repulsive and manifests itself through a term proportional to five powers of the temperature in the free energy density, is a three-loop effect.

Our calculation applies to any system with a spontaneously broken internal symmetry $\mathrm{O}(N)\to\mathrm{O}(N-1)$, provided that the corresponding leading-order effective Lagrangian can be brought to a Lorentz-invariant form. This system will be referred to as O(N) antiferromagnet. Throughout the paper, when talking about dimension, we always refer to the space-time dimension $d=d_s+1$, where d_s is the spatial dimension.

The attentive reader may particularly wonder why the quantum Heisenberg antiferromagnet,

$$\mathcal{H}=-J\sum_{n.n.}\vec{S}_m\cdot\vec{S}_n,\quad J=\mathrm{const},\tag{1.1}$$

falls into the class of O(3) antiferromagnets, i.e., represents a system described by a Lorentz-invariant leading-order effective Lagrangian. After all, the lattice structure of a solid singles out preferred directions, such that the effective Lagrangian in general is not even invariant under space rotations. In the case of a cubic lattice, however, the anisotropy only shows up at higher orders of the derivative expansion[8]—the discrete symmetries of the three-dimensional cubic crystal thus imply space rotation symmetry at leading order in the effective expansion. The same is true for an antiferromagnet defined on a square or a honeycomb lattice, which represents the system considered in this paper. Hence, the leading-order effective Lagrangian describing the quantum Heisenberg antiferromagnet on a cubic ($d=3+1$) or square/honeycomb ($d=2+1$) lattice is invariant under space rotations and can be brought to a (pseudo-)Lorentz-invariant form:[2] antiferromagnetic spin-wave excitations exhibit relativistic kinematics with the velocity of light replaced by the spin-wave velocity. As we will explain in detail later on, the spatial anisotropies which indeed start manifesting themselves at next-to-leading order in the effective Lagrangian, will not affect at all the main result of the present paper. Hence, a Lorentz-invariant framework, even at next-to-leading order of the derivative expansion, is perfectly justified in our calculation.

Goldstone's theorem, which represents the basis of the systematic effective Lagrangian method, states that, if the symmetry $G=\mathrm{O}(N)$ of the Lagrangian is spontaneously broken to $H=\mathrm{O}(N-1)$, we must have $N-1$ Goldstone bosons in the broken phase ($N\geq 2$). For $N=3$, these low-energy degrees of freedom are identified with the two spin-wave excitations—or the two independent magnon particles—in the spectrum of the O(3) antiferromagnet.

If the perturbations, which explicitly break the internal rotation symmetry O(N) of the Lagrangian, are small, the corresponding Goldstone excitations remain light and dominate the low-energy behavior of the system. The effective Lagrangian method thus also applies to antiferromagnets in weak external fields. Goldstone's theorem guarantees that the Goldstone particles interact only weakly at low energies such that a systematic perturbative expansion in the momenta and the external fields can be performed. In the present work we perturbatively evaluate the partition function in a power series of the temperature, in order to obtain low-temperature theorems for various quantities of physical interest.

We would like to emphasize that, from the effective Lagrangian perspective, the analysis of the low-energy properties of the system is approached from a unified and model-independent point of view, based on the spontaneously broken symmetry of the system. The method applies to any system where the Goldstone bosons are the only excitations without energy gap. The essential point is that the properties of these low-energy degrees of freedom and their mutual interaction are strongly constrained by the symmetries inherent in the underlying theory, such as the Heisenberg Hamiltonian—the specific nature of the underlying theory or model, however, is not important. For general pedagogic introductions to the effective Lagrangian technique see Ref. 9. Brief outlines of the method may be found in Ref. 10. For specific applications to condensed-matter systems the reader may consult Refs. 3, 4, 8, and 11–16.

Although our analysis is general, referring to any system which exhibits a spontaneously broken symmetry $\mathrm{O}(N)\to\mathrm{O}(N-1)$ and a Lorentz-invariant leading-order effective Lagrangian, our interest will primarily be devoted to the special case $N=3$, which describes the O(3) Heisenberg antiferromagnet in $d=2+1$ defined on a square or a honeycomb lattice. Here the internal O(3) spin symmetry of the isotropic Heisenberg model is spontaneously broken by the ground state which displays a nonzero staggered magnetization. This system has been widely studied in condensed-matter physics and it will be instructive to compare our results with the findings derived within the microscopic Heisenberg model. As we will see, the effective-field theory approach is by far more powerful than spin-wave theory.

Apart from our specific application concerning the partition function of the O(3) antiferromagnet in $d=2+1$ up to three-loop accuracy, we would like to point out that the effective-field theory approach to this condensed-matter system has also proven to be very efficient in other applications: In particular, in a recent publication on the constraint effective potential of the staggered magnetization of the O(3) antiferromagnet,[15] the quantitative correctness of the magnon effective-field theory has been demonstrated in great detail at per mille level accuracy by comparison with Monte Carlo simulations of the quantum Heisenberg model using the very efficient loop-cluster algorithm. At this accuracy, three-loop effects clearly start manifesting themselves as there are small discrepancies between the Monte Carlo data and the two-loop predictions of the effective-field theory. Indeed, it would be interesting to extend the finite-volume effective-field theory formulas for the constraint effective potential to three loops and to confirm the correctness of the effective-field theory approach on an even higher level of accuracy. While this finite-volume calculation may be performed in a future study, in the present work we focus on finite temperature.

The paper is organized as follows. For the sake of self-consistency, in Sec. II, we give a brief outline of the effective Lagrangian method at finite temperature. In Sec. III we present the evaluation of the partition function up to three-loop order in the perturbative expansion. The issue of renormalization is then discussed in Sec. IV. Section V contains our main results, i.e., the low-temperature series for the free energy density and other thermodynamic quantities up to three-loop order. In Sec. VI we justify why it is legitimate to use a (pseudo-)Lorentz-invariant framework in our calculation. We then compare in Sec. VII our results which apply to O(3) antiferromagnets in three dimensions with those for O(3) antiferromagnets in four dimensions. Finally, Sec. VIII contains our conclusions while some technical details concerning the renormalization and the evaluation of a specific three-loop graph are relegated to three Appendices.

II. EFFECTIVE LAGRANGIAN METHOD AT FINITE TEMPERATURE

In a Lorentz-invariant framework the construction of effective Lagrangians is straightforward:[17] one writes down the most general expression consistent with Lorentz symmetry and the internal, spontaneously broken symmetry G of the underlying model in terms of Goldstone fields $U^a(x)$, $a=1,\ldots,\dim(G)\text{-}\dim(H)$—the effective Lagrangian then consists of a string of terms involving an increasing number of derivatives or, equivalently, amounts to an expansion in powers of the momentum. Furthermore, the effective Lagrangian method allows to systematically take into account interactions which explicitly break the symmetry G of the underlying model, provided that they can be treated as perturbations.

In the particular case we are considering, the symmetry $G=\mathrm{O}(N)$ is explicitly broken by an external field. It is convenient to collect the $(N-1)$ Goldstone fields U^a in a N-dimensional vector $U^i=(U^0,U^a)$ of unit length,

$$U^i(x)U^i(x)=1, \tag{2.1}$$

and to take the constant external field along the zeroth axis, $H^i=(H,0,\ldots,0)$. The Euclidean form of the effective Lagrangian up to and including order p^4 then reads,[1]

$$\mathcal{L}_{eff}=\mathcal{L}^2_{eff}+\mathcal{L}^4_{eff},$$

$$\mathcal{L}^2_{eff}=\frac{1}{2}F^2\partial_\mu U^i\partial_\mu U^i-\Sigma_s H^iU^i,$$

$$\mathcal{L}^4_{eff}=-e_1(\partial_\mu U^i\partial_\mu U^i)^2-e_2(\partial_\mu U^i\partial_\nu U^i)^2+k_1\frac{\Sigma_s}{F^2}(H^iU^i)$$

$$\times(\partial_\mu U^k\partial_\mu U^k)-k_2\frac{\Sigma_s^2}{F^4}(H^iU^i)^2-k_3\frac{\Sigma_s^2}{F^4}H^iH^i. \tag{2.2}$$

In the momentum power counting scheme, the field $U(x)$

counts as a quantity of order 1. Derivatives correspond to one power of the momentum, $\partial_\mu \propto p$, whereas the external field H counts as a term of order p^2. Hence, at leading order ($\propto p^2$) we have two coupling constants, F and Σ_s, while at next-to-leading order ($\propto p^4$) already five constants, e_1, e_2, k_1, k_2, and k_3, show up. Note that these couplings are not fixed by symmetry—they parameterize the physics of the underlying theory and have to be determined either experimentally or in a numerical simulation. Using magnetic terminology, the square of the effective coupling constant F is the spin stiffness, while for the O(3) antiferromagnet the quantities Σ_s and H^i represent the staggered magnetization and the staggered external field, respectively.

The effective Lagrangian method provides us with a simultaneous expansion of physical quantities in powers of the momenta and of the external field. The essential point is that, to a given order in the low-energy expansion, only a finite number of coupling constants and only a finite number of graphs contribute. The leading terms stem from tree graphs, whereas loop graphs only manifest themselves at higher orders in the derivative expansion.[18]

A crucial difference with respect to the effective analysis in four space-time dimensions concerns the suppression of loops in Feynman graphs: while loops are suppressed by *two* momentum powers in four space-time dimensions, in three space-time dimensions loop corrections are suppressed by only *one* power of momentum.[19] As a consequence, the number of Feynman graphs that contribute to the perturbative expansion of the partition function up to a given order p^n, will depend on the space-time dimension. As we will see in the next section, there are fewer graphs in three dimensions that contribute up to three-loop order.

The effective Lagrangian technique can readily be extended to finite temperature. For a review of the effective Lagrangian method at nonzero temperature, see Ref. 20. For a general review of field theory at finite temperature, see Ref. 21. In the partition function, contributions of massive particles are suppressed exponentially, such that the Goldstone bosons dominate the properties of the system at low temperatures. In the power counting rules, the role of the external momenta is taken over by the temperature, which is treated as a small quantity of order p. The interaction among the Goldstone degrees of freedom in three dimensions generates corrections of order $p/F \propto T/F$, while in four dimensions, the corrections are of order $p^2/F^2 \propto T^2/F^2$.

In the effective Lagrangian framework at finite temperature, the partition function is represented as a Euclidean functional integral,[20,21]

$$\mathrm{Tr}[\exp(-\mathcal{H}/T)] = \int [dU] \exp\left(-\int_{\mathcal{T}} d^4x \mathcal{L}_{eff}\right). \quad (2.3)$$

The integration is performed over all field configurations which are periodic in the Euclidean time direction, $U(\vec{x},x_4+\beta)=U(\vec{x},x_4)$ with $\beta \equiv 1/T$. The low-temperature expansion of the partition function is obtained by considering the fluctuations of the field U around the ground state $V=(1,0,\ldots,0)$, i.e., by expanding U^0 in powers of U^a, $U^0=\sqrt{1-U^aU^a}$. The leading contribution (order p^2) contains a term quadratic in U^a which describes free (pseudo-)Goldstone bosons of mass

$$M^2 = \Sigma_s H/F^2. \quad (2.4)$$

The remainder of the effective Lagrangian is treated as a perturbation. Evaluating the Gaussian integrals in the standard manner, one arrives at a set of Feynman rules which differ from the conventional rules of the effective Lagrangian method only in one respect: the periodicity condition imposed on the Goldstone field modifies the propagator. At finite temperature, the propagator is given by

$$G(x) = \sum_{n=-\infty}^{\infty} \Delta(\vec{x},x_4+n\beta), \quad (2.5)$$

where $\Delta(x)$ is the Euclidean propagator at zero temperature. We restrict ourselves to the infinite-volume limit and evaluate the free energy density z, defined by

$$z = -T \lim_{L\to\infty} L^{-3} \ln[\mathrm{Tr}\exp(-\mathcal{H}/T)]. \quad (2.6)$$

To evaluate the graphs of the effective theory, it is convenient to use dimensional regularization, since the symmetries of the theory are preserved within this scheme. The zero-temperature propagator then reads

$$\Delta(x) = (2\pi)^{-d} \int d^dp e^{ipx}(M^2+p^2)^{-1}$$

$$= \int_0^\infty d\rho (4\pi\rho)^{-d/2} e^{-\rho M^2 - x^2/4\rho}. \quad (2.7)$$

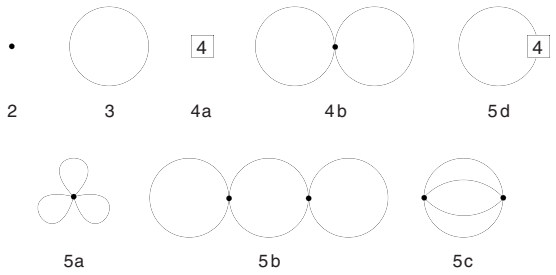

FIG. 1. Feynman graphs related to the low-temperature expansion of the partition function for an O(N) antiferromagnet up to three-loop order in dimension $d=2+1$. The numbers attached to the vertices refer to the piece of the effective Lagrangian they come from. Vertices associated with the leading term $\mathcal{L}^2_{eff}$ are denoted by a dot. Note that loops are suppressed by one momentum power in $d=2+1$.

III. FEYNMAN GRAPHS

Our aim is to evaluate the partition function of an O(N) antiferromagnet in dimension $d=2+1$ up to three-loop order—the relevant Feynman graphs are shown in Fig. 1. At leading order (order p^2), we have a tree graph involving $\mathcal{L}^2_{eff}$. The next order is p^3, where we have a one-loop graph. Remember that in three dimensions every loop leads to a suppression of one momentum power only. At order p^4 the next-

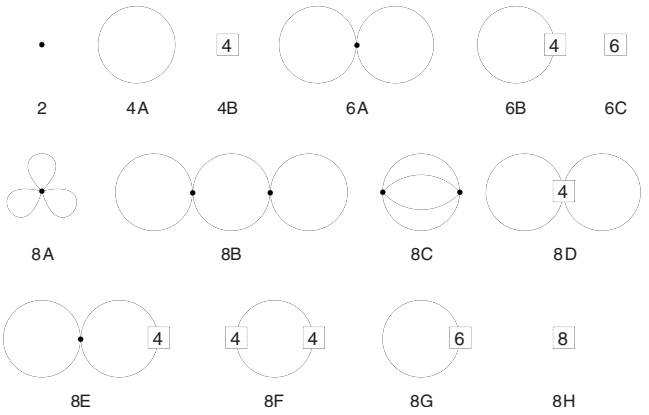

FIG. 2. Feynman graphs related to the low-temperature expansion of the partition function for an O(N) antiferromagnet up to three-loop order in dimension $d=3+1$. The numbers attached to the vertices refer to the piece of the effective Lagrangian they come from. Vertices associated with the leading term $\mathcal{L}^2_{eff}$ are denoted by a dot. Note that loops are suppressed by two momentum powers in $d=3+1$. Note also that we have used capital letters A,B,...,H in the definition of the diagrams, in order to distinguish them from the diagrams in $d=2+1$ displayed in Fig. 1, where we have used lowercase letters.

to-leading order Lagrangian $\mathcal{L}^4_{eff}$ contributes to a tree graph while the leading Lagrangian $\mathcal{L}^2_{eff}$ manifests itself in the form of a two-loop graph. The situation is more involved at order p^5, where we have three three-loop graphs with insertions from $\mathcal{L}^2_{eff}$, as well as a one-loop graph involving $\mathcal{L}^4_{eff}$. Note that higher-order pieces of the effective Lagrangian, starting with $\mathcal{L}^6_{eff}$, are not relevant for the evaluation of the partition function in $d=2+1$ at the three-loop level.

In order to compare our three-loop calculation in 2+1 dimensions with the one referring to the evaluation of the partition function for an O(N) antiferromagnet in 3+1 dimensions, we have displayed the relevant graphs for the latter case in Fig. 2. Note that loops are now suppressed by two momentum powers, which leads to 14 diagrams up to the three-loop level, whereas in three dimensions we only have eight diagrams. As we will see later on, the different loop counting and thus different organization of Feynman graphs reflects itself also in the renormalization of these graphs which turns out to be less involved in three dimensions.

Let us now consider the case $d=2+1$ and address the contributions from the relevant Feynman graphs of Fig. 1 individually. At order p^2, the tree graph involving the leading-order effective Lagrangian leads to a temperature-independent contribution,

$$z_2 = -F^2M^2. \tag{3.1}$$

At order p^3, the one-loop graph involving $\mathcal{L}^2_{eff}$, which represents the free Bose gas term, is given by

$$z_3 = -\frac{1}{2}(N-1)(4\pi)^{-3/2}\Gamma\left(-\frac{3}{2}\right)M^3 - \frac{1}{2}(N-1)g_0(M,T). \tag{3.2}$$

The function $g_0(M,T)$ is part of a set of kinematical functions $g_0(M,T)$, $g_1(M,T)$, and $g_2(M,T)$ which are associated with the d-dimensional noninteracting Bose gas and are defined by

$$g_r(M,T) = 2\int_0^\infty \frac{d\rho}{(4\pi\rho)^{d/2}}\rho^{r-1} \times \exp(-\rho M^2)\sum_{n=1}^{\infty}\exp(-n^2/4\rho T^2). \tag{3.3}$$

There are two graphs at order p^4. The tree graph 4a involves two coupling constants from the next-to-leading order Lagrangian,

$$z_{4a} = -(k_2+k_3)M^4, \tag{3.4}$$

while the two-loop graph 4b leads to a temperature-dependent contribution

$$z_{4b} = \frac{1}{8}(N-1)(N-3)\frac{M^2}{F^2}(G_1)^2. \tag{3.5}$$

The expression G_1 denotes the value of the thermal propagator at the origin

$$G_1 \equiv G(x)|_{x=0}. \tag{3.6}$$

The situation is more complicated at order p^5, where we have four graphs: The three-loop graphs 5a–5c, involving the leading-order effective Lagrangian $\mathcal{L}^2_{eff}$, as well as a one-loop graph with a vertex from the next-to-leading order Lagrangian $\mathcal{L}^4_{eff}$.

Graph 5a factorizes into a term which only involves the thermal propagator at the origin,

$$z_{5a} = \frac{1}{16}(N+1)(N-1)(N-5)\frac{M^2}{F^4}(G_1)^3. \tag{3.7}$$

Likewise, graph 5b exclusively contains propagators or derivatives thereof evaluated at the origin,

$$z_{5b} = -\frac{1}{4}(N-1)(N-3)\frac{M^2}{F^4}(G_1)^3 - \frac{1}{16}(N-1)(N-3)^2\frac{M^4}{F^4}(G_1)^2G_2. \tag{3.8}$$

The quantity G_2 corresponds to an integral over the torus $\mathcal{T}=\mathcal{R}^{d_s}\times S^1$ with circle S^1 defined by $-\beta/2\le x_4\le\beta/2$, and reads

$$G_2 = \int_{\mathcal{T}} d^dx\{G(x)\}^2. \tag{3.9}$$

This integral can be expressed in terms of the derivative of the propagator at the origin with respect to the mass,

$$G_2 = -\frac{dG_1}{dM^2}. \tag{3.10}$$

Graph 5c leads to integrals over products of four propagators. Integrating by parts, they can be brought to the form

$$z_{5c} = \frac{1}{48}(N-1)(N-3)\frac{M^4}{F^4}J_1 - \frac{1}{4}(N-1)(N-2)\frac{1}{F^4}J_2 + \frac{1}{6}N(N-1)\frac{M^2}{F^4}(G_1)^3, \tag{3.11}$$

where the functions J_1 and J_2 are given by

$$J_1 = \int_{\mathcal{T}} d^d x \{G(x)\}^4,$$

$$J_2 = \int_{\mathcal{T}} d^d x \{\partial_\mu G(x) \partial_\mu G(x)\}^2. \tag{3.12}$$

Finally, the one-loop graph 5d with an insertion from $\mathcal{L}^4_{eff}$ yields

$$z_{5d} = (N-1)(k_2 - k_1)\frac{M^4}{F^2}G_1. \tag{3.13}$$

Collecting all the pieces, we obtain the following expression for the free energy density of an O(N) antiferromagnet in dimension $d=2+1$ up to and including three loops,

$$\begin{aligned} z = &- F^2M^2 - \frac{1}{2}(N-1)(4\pi)^{-3/2}\Gamma\left(-\frac{3}{2}\right)M^3 \\ &- \frac{1}{2}(N-1)g_0(M,T) - (k_2+k_3)M^4 \\ &+ \frac{1}{8}(N-1)(N-3)\frac{M^2}{F^2}(G_1)^2 + \frac{1}{48}(N-1)(N-3) \\ &\times(3N-7)\frac{M^2}{F^4}(G_1)^3 - \frac{1}{16}(N-1)(N-3)^2\frac{M^4}{F^4}(G_1)^2G_2 \\ &+ \frac{1}{48}(N-1)(N-3)\frac{M^4}{F^4}J_1 - \frac{1}{4}(N-1)(N-2)\frac{1}{F^4}J_2 \\ &+ (N-1)(k_2-k_1)\frac{M^4}{F^2}G_1 + \mathcal{O}(p^6). \end{aligned} \tag{3.14}$$

Note that the quantities above involve the bare mass M of the (pseudo-)Goldstone bosons given in Eq. (2.4). The thermodynamics of the antiferromagnet is contained in the functions g_0, G_1, G_2, J_1, and J_2 which depend in a nontrivial manner on the ratio M/T. In the following section, we will take care of the singularities contained in the above expression and derive the low-temperature expansion for the free energy density.

IV. DIVERGENCES AT $d=2+1$ AND RENORMALIZATION

In order to analyze the divergences in the limit $d \to 3$, we split the thermal propagator into two pieces,

$$G(x) = \Delta(x) + \bar{G}(x), \tag{4.1}$$

where $\Delta(x)$ represents the propagator at zero temperature. At the origin, we have

$$G_1 = 2M^2\lambda + g_1(M,T),$$

$$G_2 = (2-d)\lambda + g_2(M,T). \tag{4.2}$$

The temperature-dependent quantities $g_r(M,T)$, defined in Eq. (3.3), are smooth functions in the limit $d \to 3$. The temperature-independent contributions involve the parameter λ,

$$\lambda = \frac{1}{2}(4\pi)^{-d/2}\Gamma\left(1-\frac{d}{2}\right)M^{d-4}. \tag{4.3}$$

Remarkably, λ is finite in the limit $d \to 3$,

$$\lambda = -\frac{1}{8\pi M}. \tag{4.4}$$

On the other hand, in the limit $d \to 4$ the parameter λ contains a pole due to the singular behavior of the gamma function. Accordingly, logarithmic divergences in the ultraviolet show up in four space-time dimensions, such that the next-to-leading order effective constants will undergo a logarithmic renormalization in $d=3+1$. For the moment, however, we focus on the case $d=2+1$.

In order to remove the singularities in the remaining integrals J_1 and J_2, as we show in Appendix A, it suffices to subtract counterterms of the form $c_1+c_2g_1(M,T)$ and $c_3+c_4g_1(M,T)$, respectively,

$$\bar{J}_1 = J_1 - c_1 - c_2 g_1(M,T),$$

$$\bar{J}_2 = J_2 - c_3 - c_4 g_1(M,T), \tag{4.5}$$

where the constants c_i are singular functions of the dimension d. While the quantities c_1 and c_3 renormalize the vacuum energy, c_2 and c_4 renormalize the mass M (see below).

We now insert the decompositions, Eqs. (4.2) and (4.5), into the free energy density, Eq. (3.14), and discuss the various pieces therein. All contributions which are independent of the temperature,

$$\begin{aligned} z_0 = &- F^2M^2 - \frac{1}{12\pi}(N-1)M^3 - (k_2+k_3)M^4 + \frac{1}{128\pi^2}(N-1) \\ &\times(N-3)\frac{M^4}{F^2} - \frac{1}{6144\pi^3}(N-1)(N-3)(9N-23)\frac{M^5}{F^4} \\ &+ \frac{1}{48}(N-1)(N-3)\frac{M^4}{F^4}c_1 - \frac{1}{4}(N-1)(N-2)\frac{1}{F^4}c_3 \\ &- \frac{1}{4\pi}(N-1)(k_2-k_1)\frac{M^5}{F^2} + \mathcal{O}(p^6), \end{aligned} \tag{4.6}$$

merely renormalize the vacuum energy.

Next, we consider all terms in the free energy density, Eq. (3.14), which are linear in the kinematical functions $g_r(M,T)$. In Appendix B we show that these contributions can be merged into a single term proportional to $g_0(M_\pi,T)$ by renormalizing the mass, $M \to M_\pi$, according to

$$M_\pi^2 = M^2 + (N-3)\lambda\frac{M^4}{F^2} + \left\{2(k_2-k_1) + \frac{b_1}{F^2} + \frac{b_2\lambda^2 M^2}{F^2}\right\}\frac{M^4}{F^2} + \mathcal{O}(M^5). \tag{4.7}$$

The quantity b_1 is related to the singularities contained in the coefficients c_2 and c_4. We thus see that the divergences in b_1, originating from the three-loop graph 5c, are absorbed into the combination k_2-k_1 (stemming from the one-loop graph 5d) of next-to-leading order effective constants. After mass renormalization, the only surviving term linear in the kinematical function is the contribution from the free energy density of noninteracting magnons given by

$$-\frac{1}{2}(N-1)g_0(M_\pi,T), \tag{4.8}$$

which now depends on the renormalized mass M_π.

Finally we have to take care of the terms quadratic and cubic in the functions $g_r(M,T)$, which is also done in Appendix B. We are then left with the following expression for the free energy density of an O(N) antiferromagnet in three dimensions,

$$z = z_0 - \frac{1}{2}(N-1)g_0 + \frac{1}{8}(N-1)(N-3)\frac{M_\pi^2}{F^2}(g_1)^2 - \frac{1}{128\pi}(N-1)(N-3)(5N-11)\frac{M_\pi^3}{F^4}(g_1)^2 + \frac{1}{48}(N-1)(N-3)(3N-7)\frac{M_\pi^2}{F^4}(g_1)^3 - \frac{1}{16}(N-1)(N-3)^2\frac{M_\pi^4}{F^4}(g_1)^2 g_2 + \frac{Q}{F^4} + \mathcal{O}(p^6), \tag{4.9}$$

where we have defined the function $Q(M_\pi,T)$ by

$$Q \equiv \frac{1}{48}(N-1)(N-3)M_\pi^4\bar{J}_1 - \frac{1}{4}(N-1)(N-2)\bar{J}_2. \tag{4.10}$$

Expression (4.9) for the free energy density is free of divergences and only involves the physical mass M_π. In particular, the kinematical functions are defined as $g_r = g_r(M_\pi,T)$.

For dimensional reasons, the thermodynamic functions in Eq. (4.9) are of the form $T^p f(\tau)$, where τ is the dimensionless ratio

$$\tau = \frac{T}{M_\pi}. \tag{4.11}$$

Explicitly, in $d=2+1$ they are given by

$$g_0 = T^3 h_0(\tau), \quad g_1 = T h_1(\tau), \quad g_2 = \frac{1}{T}h_2(\tau), \qquad Q = T^5 q(\tau), \tag{4.12}$$

such that the free energy density can be written as

$$z = z_0 - \frac{1}{2}(N-1)h_0(\tau)T^3 + \frac{1}{8}(N-1)(N-3)\frac{1}{F^2\tau^2}h_1(\tau)^2T^4 - \frac{1}{128\pi}(N-1)(N-3)(5N-11)\frac{1}{F^4\tau^3}h_1(\tau)^2T^5 + \frac{1}{48}(N-1)(N-3)(3N-7)\frac{1}{F^4\tau^2}h_1(\tau)^3T^5 - \frac{1}{16}(N-1)(N-3)^2\frac{1}{F^4\tau^4}h_1(\tau)^2h_2(\tau)T^5 + \frac{1}{F^4}q(\tau)T^5 + \mathcal{O}(T^6). \tag{4.13}$$

This expression for the free energy density of an O(N) antiferromagnet in $2+1$ dimensions represents the basic result of our paper. The ratio $\tau = T/M_\pi$ can take any value, as long as the quantities T and M_π themselves are small compared to the intrinsic scale Λ of the theory which, in the case of the O(3) antiferromagnet, may be identified with the exchange integral J of the Heisenberg model (1.1).

Remarkably, for $N=3$—the quantum Heisenberg antiferromagnet on a square lattice—most of the terms drop out and we are left with the following simple expression for the free energy density of the O(3) antiferromagnet in $d=2+1$,

$$z = z_0 - h_0(\tau)T^3 + \frac{1}{F^4}q(\tau)T^5 + \mathcal{O}(T^6) \quad (N=3). \tag{4.14}$$

While the term cubic in the temperature corresponds to the free Bose gas, the term proportional to five powers of the temperature represents the leading contribution due to the spin-wave interaction. Note that for this special case ($N=3$), the function $q(\tau)$ defined in Eq. (4.12) only involves the contribution proportional to $\bar{J}_2$.

V. LOW-TEMPERATURE SERIES FOR THE O(3) ANTIFERROMAGNET IN $d=2+1$

With the representation, Eq. (4.14), for the free energy density of the O(3) antiferromagnet in $2+1$ dimensions, we are now able to discuss various thermodynamic quantities for this system. We are particularly interested in the limit $T \gg M_\pi$ which we implement by holding T fixed and sending M_π (or, equivalently, the external field H) to zero. Since we keep the fixed T small compared to the intrinsic scale Λ of the underlying theory, we do not leave the domain of validity of the low-temperature expansion.

Because the system is homogeneous, the pressure is given by the temperature-dependent part of the free energy density,

$$P = z_0 - z = h_0(\tau)T^3 - \frac{1}{F^4}q(\tau)T^5 + \mathcal{O}(T^6). \tag{5.1}$$

The nontrivial dependence of the quantity P on the ratio $\tau = T/M_\pi$ is contained in the functions $h_0(M_\pi,T)$ and $q(M_\pi,T)$, which are defined in Eqs. (3.3) and (4.12). For the function $h_0(M_\pi,T)$ an analytical expression can be provided in the limit $T \gg M_\pi$ (see Appendix C),

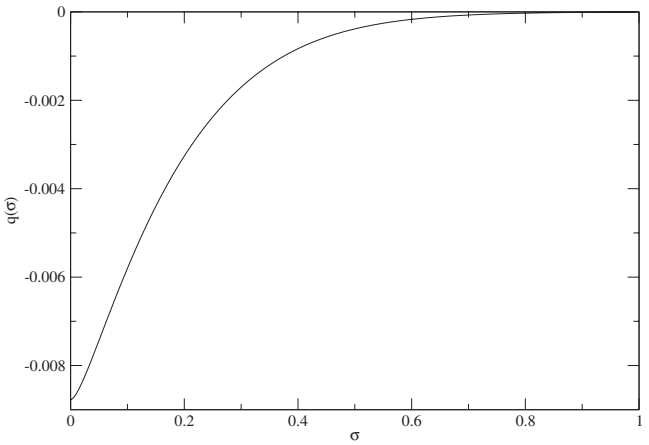

FIG. 3. The function $q(\sigma)$ for $N=3$, where σ is the dimensionless parameter $\sigma=M_\pi/2\pi T=1/2\pi\tau$, introduced in Ref. 22.

$$h_0^{d=3}(\tau)=\frac{1}{\pi}\left[\zeta(3)-\frac{1}{4}\frac{M_\pi^2}{T^2}+\frac{1}{4}\frac{M_\pi^2}{T^2}\ln\frac{M_\pi^2}{T^2}-\frac{1}{6}\frac{M_\pi^3}{T^3}+\frac{1}{96}\frac{M_\pi^4}{T^4}+\mathcal{O}\left(\frac{M_\pi}{T}\right)^6\right]. \tag{5.2}$$

The function $q(M_\pi,T)$, on the other hand, we have evaluated numerically, using the representation for $\bar{J}_2$ given in Appendix A—a plot of is provided in Fig. 3. Still, in the limit $T\gg M_\pi$, the function may be parameterized by

$$q(\tau)=q_1+\mathcal{O}\left(\frac{M_\pi^2}{T^2}\ln\frac{M_\pi^2}{T^2}\right),\quad \tau=\frac{T}{M_\pi}, \tag{5.3}$$

where the coefficient q_1 is a real number which takes the value

$$q_1=-0.008779. \tag{5.4}$$

Making use of the above representations for $h_0(M_\pi,T)$ and $q(M_\pi,T)$, in the limit $T\gg M_\pi$ the pressure takes the form

$$P=\frac{\zeta(3)}{\pi}T^3\left[1-\frac{\pi q_1}{\zeta(3)}\frac{T^2}{F^4}+\mathcal{O}(T^3)\right]\approx 0.3826T^3\left[1+0.02294\frac{T^2}{F^4}+\mathcal{O}(T^3)\right]. \tag{5.5}$$

The corresponding expressions for the energy density u, for the entropy density s, and for the heat capacity c_V for the O(3) antiferromagnet in 2+1 dimensions, are readily worked out from the thermodynamic relations

$$s=\frac{\partial P}{\partial T},\quad u=Ts-P,\quad c_V=\frac{\partial u}{\partial T}=T\frac{\partial s}{\partial T} \tag{5.6}$$

with the result

$$u=\frac{2\zeta(3)}{\pi}T^3\left[1-\frac{2\pi q_1}{\zeta(3)}\frac{T^2}{F^4}+\mathcal{O}(T^3)\right]\approx 0.7653T^3\left[1+0.04589\frac{T^2}{F^4}+\mathcal{O}(T^3)\right],$$

$$s=\frac{3\zeta(3)}{\pi}T^2\left[1-\frac{5\pi q_1}{3\zeta(3)}\frac{T^2}{F^4}+\mathcal{O}(T^3)\right]\approx 1.1479T^2\left[1+0.03824\frac{T^2}{F^4}+\mathcal{O}(T^3)\right],$$

$$c_V=\frac{6\zeta(3)}{\pi}T^2\left[1-\frac{10\pi q_1}{3\zeta(3)}\frac{T^2}{F^4}+\mathcal{O}(T^3)\right]\approx 2.2958T^2\left[1+0.07648\frac{T^2}{F^4}+\mathcal{O}(T^3)\right]. \tag{5.7}$$

The respective first terms in the above series represent the free Bose gas contribution which originates from a one-loop graph. The effective interaction among the Goldstone bosons only manifests itself through a term of order T^5 in the pressure related to a three-loop graph. Interestingly, the coefficient q_1 is negative, such that the magnon-magnon interaction in the O(3) antiferromagnet in $d=2+1$ is repulsive at low temperatures. It is remarkable that the coefficient of the interaction term in these series is fully determined by the symmetries inherent in the leading-order effective Lagrangian, and does not involve any next-to-leading order coupling constants from $\mathcal{L}_{eff}^4$, reflecting the anisotropies of the square lattice or the Lorentz-noninvariant nature of the quantum Heisenberg antiferromagnet defined on a square or a honeycomb lattice—the symmetry is thus very restrictive in $d=2+1$. Note that there is no interaction term of order T^4 in the pressure: the two-loop contribution z_{4b} is proportional to $N-3$ and thus vanishes for the O(3) antiferromagnet, irrespective of the actual value of the ratio $\tau=T/M_\pi$.

The fact that an interaction term proportional to four powers of the temperature does not show up in the temperature expansion for the pressure of the O(3) antiferromagnet in the limit $T\gg M_\pi$ was already pointed out in Ref. 8: this was an effective Lagrangian calculation that operated on the two-loop level. We are not aware of any microscopic calculation that aimed at this accuracy. Moreover, our result that the leading contribution of the magnon-magnon interaction in the pressure is repulsive and of order T^5 requires a three-loop calculation on the effective level, performed in the present study—it is probably fair to say that this accuracy is beyond the reach of any realistic microscopic calculation based on spin-wave theory.

In fact, as pointed out in Ref. 8, there were inconsistencies between the results obtained by spin-wave theory, Schwinger boson mean-field theory and Monte Carlo simulations, already with respect to the very leading term ($\propto T^3$) in the temperature expansion of the energy density.[23–25] The error was later attributed to some numerical problems in solving the equations arising in Schwinger boson mean-field theory. The systematic effective Lagrangian method, which approaches the problem from a unified and model-

independent perspective based on the symmetries of the underlying theory, thus clearly proves to be superior to these conventional condensed-matter techniques.

As demonstrated in a recent publication on the constraint effective potential of the staggered magnetization of the O(3) antiferromagnet,[15] three-loop effects clearly start manifesting themselves, as there are small discrepancies between the very precise Monte Carlo data and the two-loop predictions of the effective-field theory. Indeed, it would be interesting to extend the finite-volume effective-field theory formulas for the constraint effective potential to three loops, in order to confirm the correctness of the effective-field theory approach on an even higher level of accuracy and to extract the numerical values of some combinations of effective next-to-leading order coupling constants. Although nontrivial, this would certainly be feasible within the framework of the systematic magnon effective-field theory.

We now make an important comment on the range of validity of the above low-temperature series. After all, we are considering the limit $T \gg M_\pi$, which we have implemented by holding T fixed and sending M_π, or, equivalently, the external field H, to zero. However, following Mermin and Wagner,[26] there is no spontaneous symmetry breaking at any finite temperature in the O(3)-invariant Heisenberg model. Accordingly, there are no massless magnons in the low-energy spectrum at any finite temperature. Rather, the magnons pick up an exponentially small mass. The argument of the exponential is proportional to the inverse temperature,

$$m = \left(\frac{8}{e}\right) 2\pi F^2 \exp\left[-\frac{2\pi F^2}{T}\right]\left\{1 + \frac{1}{2}\frac{T}{2\pi F^2} + \mathcal{O}\left(\frac{T^2}{F^4}\right)\right\}, \tag{5.8}$$

as derived in Refs. 5 and 27. Strictly speaking, it is therefore not legitimate to switch off the external field H completely because the above calculation does not take into account the nonperturbative effect of m. However, the corrections due to the nonperturbatively generated mass gap are so tiny that they cannot manifest themselves in the above power series. In order to verify this claim, we now estimate the order of magnitude of these corrections.

The above low-temperature series are valid as long as the correlation length of the Goldstone bosons, $\xi = 1/M_\pi$ is much smaller than the nonperturbatively generated correlation length $\xi_{np} = 1/m$, let us say,

$$\frac{1}{1000} = \frac{\xi}{\xi_{np}} = \frac{8}{e}\frac{2\pi F^2}{T}\frac{T}{M_\pi}\exp\left[-\frac{2\pi F^2}{T}\right], \tag{5.9}$$

where we have used Eq. (5.8). For the Heisenberg antiferromagnet in $d=2+1$, the spin stiffness F^2 has been determined very precisely in Monte Carlo simulations.[15,28] In units of the exchange integral J it takes the value $F^2 = 0.1808(4)J$, such that the quantity $2\pi F^2$ is on the order of J. Now the exchange integral defines a scale in the underlying theory and for the effective expansion to be consistent, the temperature has to be small with respect to this scale. Assuming that

$$\frac{T}{2\pi F^2} = \frac{1}{100}, \tag{5.10}$$

relation (5.9) then yields the ratio

$$\frac{M_\pi}{T} \approx 10^{-38}. \tag{5.11}$$

Remember that, in the above low-temperature series, we have implemented the limit $T \gg M_\pi$ by holding T fixed and sending M_π to zero. We thus see that, in principle, we cannot completely switch off the mass M_π—rather, we start running into trouble as soon as the ratio M_π/T is on the order of the above value. However, the error introduced is indeed very small: the leading one-loop contribution in the free energy density, according to Eqs. (4.9) and (5.2) is

$$\frac{1}{\pi}\frac{1}{4}\frac{M_\pi^2}{T^2}\left[1 - \ln\frac{M_\pi^2}{T^2}\right] \approx 10^{-75}, \tag{5.12}$$

which is extremely small also with respect to the three-loop contributions in Eq. (5.5). We thus confirm that the corrections due to the nonperturbatively generated mass gap are so tiny that they cannot manifest themselves in the above low-temperature expansions for the thermodynamic quantities. In other words, the subtleties raised by the Mermin-Wagner theorem in $d=2+1$ are not relevant for our calculation.

While our effective calculation is restricted to the regime $\xi \ll \xi_{np}$, the regime $\xi \gg \xi_{np}$, is perfectly well accessible also with effective-field theory methods. However, one has to resort to a different type of perturbative expansion. A similar situation occurs when one considers finite-size effects: when the Goldstone boson mass is small compared to the inverse size of the box, a different effective expansion scheme, the so-called ϵ expansion, applies. Indeed, various problems within this framework have been investigated in detail.[29–32]

VI. JUSTIFICATION OF THE LORENTZ-INVARIANT FRAMEWORK

In this section we would like to explain why it is justified to use a Lorentz-invariant framework in our calculation. We have seen that anisotropies induced by a cubic or a square lattice do not affect the leading-order effective Lagrangian, such that $\mathcal{L}_{eff}^2$ can be written in a Lorentz-invariant form, where the spin-wave velocity takes over the role of the velocity of light: the accidental O(3) space rotation symmetry at the $\mathcal{L}_{eff}^2$ level implies (pseudo-)Lorentz invariance. On the other hand, the anisotropies related to the lattice structure do show up in the next-to-leading order effective Lagrangian $\mathcal{L}_{eff}^4$. Now, in our three-loop calculation of the partition function in $d=2+1$ the only temperature-dependent diagram involving $\mathcal{L}_{eff}^4$ is the one-loop diagram shown in 5d of Fig. 1, which is quadratic in the magnon field. Indeed, here we have a new term due to the lattice anisotropies, also contributing to the diagram. The respective term,

$$\sum_{s=1,2} \partial_s \partial_s U^i \partial_s \partial_s U^i, \tag{6.1}$$

is invariant under the 90° spatial rotation symmetry of the square lattice but not invariant under continuous O(3) space

rotations. Interestingly, this term is absent in the case of the honeycomb lattice, as it is not allowed by the 60° rotation symmetry.

However, both for the square and the honeycomb lattice there are additional terms showing up at next-to-leading order: if we consider an O(3) symmetric, i.e., space-rotation symmetric Lagrangian $\mathcal{L}^4_{eff}$—and not a Lorentz-invariant Lagrangian $\mathcal{L}^4_{eff}$ as we have done so far—there are further terms like

$$\Delta U^i \Delta U^i, \quad H^i U^i \partial_r U^k \partial_r U^k, \tag{6.2}$$

that also have to be taken into account in $\mathcal{L}^4_{eff}$. The essential observation, however, is that all these Lorentz-noninvariant extra terms in Eqs. (6.1) and (6.2) contributing to the one-loop graph 5d merely modify mass renormalization or give rise to higher-order corrections of the dispersion law,

$$\omega(\vec{k}) = v|\vec{k}| + \mathcal{O}(\vec{k}^3), \tag{6.3}$$

but cannot manifest themselves in the magnon-magnon interaction up to the order p^5 considered in the present work. Although they give rise to an additional term in the free energy density involving five powers of the temperature, this is a purely kinematical effect related to the one-loop graph 5d—the leading contribution due to the magnon-magnon interaction, also of order T^5, will not be affected. Hence, our main result regarding the weakness and the repulsive character of the magnon-magnon interaction in the O(3) antiferromagnet in $d=2+1$ perfectly well applies to the quantum Heisenberg antiferromagnet defined on a square or a honeycomb lattice.

Apart from these anisotropies induced by the lattice, we have to consider a second type of cutoff effects. While the present three-loop calculation was performed in the infinite-volume limit, in Ref. 8 the two-loop calculation for the O(N) antiferromagnet in $d=2+1$ was presented in a combined effective expansion at finite temperature as well as finite volume. The corresponding Fourier sums occurring, e.g., in the propagator will depend on a finite cutoff. However, the authors showed[33] that these momentum sums in the dominant one-loop graph 3 (see Fig. 1) only start manifesting themselves at order p^5. The noninteracting part of order p^5 is thus affected by a finite cutoff due to momentum sums, much like it depends on the other type of cutoff effects induced by the anisotropies of the square lattice.

The striking point, however, is that the momentum sums in the relevant three-loop interaction graph manifest themselves beyond order p^5. Therefore, the effective repulsive interaction term proportional to T^5 does not depend on any type of cutoff effects.

VII. ANTIFERROMAGNETS IN 2+1 AND 3+1 DIMENSIONS: STRUCTURE OF THE LOW-TEMPERATURE SERIES

In this section we want to compare the low-temperature series for antiferromagnets in 2+1 and 3+1 dimensions, pointing out differences as well as similarities. The effective Lagrangian method is ideally suited to understand the structure of these low-temperature series, as it adopts a unified perspective based on symmetry considerations. We first discuss the situation for arbitrary N and then consider the special case $N=3$, which describes the O(3)-invariant quantum Heisenberg antiferromagnet on a square or a honeycomb lattice.

As we have discussed in Sec. III, loops in four dimensions are suppressed by two momentum powers, whereas in three dimensions they are suppressed by one power of momentum only. Consequently, the organization of the loop expansion for the partition function depends on the space-time dimension and reflects itself also in the number of Feynman diagrams that have to be evaluated. Up to the three-loop level, we have the 14 diagrams in four dimensions, displayed in Fig. 2—in three dimensions there are only eight, displayed in Fig. 1. In particular, in $d=2+1$, there are no two-loop graphs involving the next-to-leading order Lagrangian $\mathcal{L}^4_{eff}$. Moreover, contributions from $\mathcal{L}^6_{eff}$ or $\mathcal{L}^8_{eff}$ are not needed in $d=2+1$. One thus notices that the restrictions imposed by symmetry are extremely strong in $d=2+1$: up to the three-loop level, no effective coupling constants from $\mathcal{L}^6_{eff}$ or $\mathcal{L}^8_{eff}$ enter the calculation and the couplings in $\mathcal{L}^4_{eff}$—as we have seen—do not affect at all the spin-wave interaction part in the free energy density.

Another immediate consequence of the dimension-dependent loop counting is the fact that interactions among antiferromagnetic magnons in $d=2+1$ generate corrections of order $p/F \propto T/F$, whereas in $d=3+1$ these corrections are of order $p^2/F^2 \propto T^2/F^2$. The low-temperature series for the various thermodynamic quantities are thus expected to proceed in steps of one power of T in $d=2+1$ and in steps of T^2 in $d=3+1$—we will come back to this point below.

We now briefly review the relevant results for an O(N) antiferromagnet in 3+1 dimensions—details of the calculation can be found in Ref. 4. The formula for the pressure takes the form

$$P = \frac{1}{2}(N-1)g_0 + 4\pi a(g_1)^2 + \pi g\left[b - \frac{j}{\pi^3 F^4}\right] + \mathcal{O}(p^{10}) \quad (d=3+1). \tag{7.1}$$

The temperature dependence is contained in the kinematical functions $g_r(M_\pi, T)$ and in $j(M_\pi, T)$. In the limit $H \to 0$ (or, equivalently, $T \gg M_\pi$) we are interested in, analytical expressions for the functions g_0, g_1, and g can be provided (see Ref. 22 or Appendix C),

$$g_0(M_\pi, T) = \frac{\pi^2}{45}T^4\left[1 - \frac{15}{4\pi^2}\frac{M_\pi^2}{T^2} + \frac{15}{2\pi^3}\frac{M_\pi^3}{T^3} + \frac{45\left(\gamma - \frac{3}{4} - \ln 4\pi\right)}{16\pi^4}\frac{M_\pi^4}{T^4} + \frac{45}{32\pi^4}\frac{M_\pi^4}{T^4}\ln\frac{M_\pi^2}{T^2} + \mathcal{O}\left(\frac{M_\pi}{T}\right)^6\right], \quad (d=3+1),$$

$$g_1(M_\pi,T) = \frac{1}{12}T^2\left[1 - \frac{3}{\pi}\frac{M_\pi}{T} + \mathcal{O}\left(\frac{M_\pi^2}{T^2}\ln\frac{M_\pi}{T}\right)\right],$$

$$g(M_\pi,T) = \frac{1}{675}\pi^4 T^8\left[1 - \frac{15}{4\pi^2}\frac{M_\pi^2}{T^2} + \mathcal{O}\left(\frac{M_\pi}{T}\right)^3\right], \quad (7.2)$$

whereas the function j, containing the three-loop contribution from graph 8C, has to be evaluated numerically,

$$j = \nu\ln\frac{T}{M_\pi} + j_1 + j_2\frac{M_\pi^2}{T^2} + \mathcal{O}\left(\frac{M_\pi}{T}\right)^3,$$

$$\nu \equiv \frac{5(N-1)(N-2)}{48}. \quad (7.3)$$

The coefficients j_1 and j_2 in this expansion are real numbers. Note that the function $j(\tau)$ diverges logarithmically in the limit $H\to 0$. It should be pointed out that the renormalized or physical mass M_π in $d=3+1$ is given by

$$M_\pi^2 = M^2 + \{(N-3)\lambda + 2(k_2-k_1)\}\frac{M^4}{F^2} + c\frac{M^6}{F^4} + \mathcal{O}(M^8) \quad (d=3+1), \quad (7.4)$$

which is different from the analogous expression (4.7) in $d=2+1$, due to the different loop counting. Without going into details, we just mention that the quantity λ, according to Eq. (4.3), is divergent in $d=3+1$ and that the corresponding singularity occurring in the two-loop graph 6A (see Fig. 2) is absorbed into the combination k_2-k_1 of next-to-leading order coupling constants originating from graph 6B. The absorbtion of the divergences showing up in the various graphs of order p^8, on the other hand, even involves a coupling constant of $\mathcal{L}_{eff}^6$ stemming from graph 8G, which is contained in the quantity c of Eq. (7.4).

Finally, the constants a and b in the pressure, Eq. (7.1), involve the scales H_a and H_b,

$$a = -\frac{(N-1)(N-3)}{32\pi}\frac{\Sigma_s H}{F^4} - \frac{(N-1)^3}{256\pi^3}\frac{(\Sigma_s H)^2}{F^8}\ln\frac{H}{H_a},$$

$$b = -\frac{5(N-1)(N-2)}{96\pi^3 F^4}\ln\frac{H}{H_b}, \quad (7.5)$$

which are related to coupling constants of $\mathcal{L}_{eff}^4$ (for details see the appendix in Ref. 4). The first term in a, linear in the external field H, originates from the two-loop graph 6A. The logarithmic contributions in a and b involving the two scales H_a and H_b, originate from two-loop graphs with insertions from $\mathcal{L}_{eff}^4$. Note that in $d=2+1$ these two-loop graphs are already beyond the next-to-next-to-leading order considered in the present paper.

Equipped with the above formulas, the low-temperature expansion of the pressure for an O(N) antiferromagnet in $d=3+1$ in the limit $H\to 0$ amounts to

$$P = \frac{1}{90}\pi^2(N-1)T^4\left[1 + \frac{N-2}{72}\frac{T^4}{F^4}\ln\frac{T_p}{T} + \mathcal{O}(T^6)\right] \quad (d=3+1). \quad (7.6)$$

The first contribution represents the free Bose gas term which originates from a one-loop graph, whereas the effective interaction among the Goldstone bosons, remarkably, only manifests itself through a term of order T^8. This contribution contains a logarithm, characteristic of the effective Lagrangian method in four space-time dimensions, which involves a scale, T_p, related to H_b (see the appendix in Ref. 4). The occurrence of a scale involving coupling constants from $\mathcal{L}_{eff}^4$ is a consequence of the space-time dimension $d=3+1$: in four dimensions the parameter λ, defined in Eq. (4.3), contains a pole, which can be absorbed into coupling constants of $\mathcal{L}_{eff}^4$ by a suitable logarithmic renormalization. Note that the divergences in the function j, Eq. (7.3), and in the constant b, Eq. (7.5), cancel, such that the remaining expression involving the scale T_p is well defined in the limit $H\to 0$.

At low temperatures, the logarithm $\ln[T_p/T]$ in the pressure, Eq. (7.6), is positive, such that the interaction among the Goldstone bosons in $d=3+1$, in the absence of an external field H, is repulsive, much like in $d=2+1$. The symmetries in $d=3+1$, however, are somewhat less restrictive than in $d=2+1$, where the interaction term—the last term in Eq. (4.13) involving the function $q(\tau)$—is unambiguously determined by the coupling constant F of the leading-order effective Lagrangian: in $d=3+1$, next-to-leading order effective constants from $\mathcal{L}_{eff}^4$ do show up in the scale T_p. Still, the symmetry is also rather restrictive in $d=3+1$, as it unambiguously fixes the coefficient in front of the logarithm in terms of the coupling constant F. Note that there is no term of order T^6 in the above series for the pressure. This is due to the fact that the respective two-loop contribution (graph 6A, Fig. 2.) in Eq. (7.1) is proportional to the constant a that vanishes for a zero external field.

Finally, the energy density u, the entropy density s, and the heat capacity c_V in the limit $H\to 0$ are given by

$$u = \frac{1}{30}\pi^2(N-1)T^4\left[1 + \frac{N-2}{216}\frac{T^4}{F^4}\left(7\ln\frac{T_p}{T} - 1\right) + \mathcal{O}(T^6)\right],$$

$$s = \frac{2}{45}\pi^2(N-1)T^3\left[1 + \frac{N-2}{288}\frac{T^4}{F^4}\left(8\ln\frac{T_p}{T} - 1\right) + \mathcal{O}(T^6)\right] \quad (d=3+1),$$

$$c_V = \frac{2}{15}\pi^2(N-1)T^3\left[1 + \frac{N-2}{864}\frac{T^4}{F^4}\left(56\ln\frac{T_p}{T} - 15\right) + \mathcal{O}(T^6)\right]. \quad (7.7)$$

Note that the limit $H\to 0$ can readily be taken in $d=3+1$ since the Mermin-Wagner theorem does not apply here: there are no exponentially small nonperturbative corrections in the above low-temperature series. On general power counting grounds one would expect the low-temperature series to proceed in steps of T^2 in $3+1$ dimensions. However, as for the pressure before, there are no correction terms proportional to,

e.g., six powers of the temperature in the internal energy because the constant a vanishes in the limit $H \to 0$.

For the specific case $N=3$, the above series for the thermodynamic quantities take the form

$$P = \frac{1}{45}\pi^2 T^4 \left[1 + \frac{1}{72}\frac{T^4}{F^4}\ln\frac{T_p}{T} + \mathcal{O}(T^6) \right],$$

$$u = \frac{1}{15}\pi^2 T^4 \left[1 + \frac{1}{216}\frac{T^4}{F^4}\left(7\ln\frac{T_p}{T} - 1 \right) + \mathcal{O}(T^6) \right],$$

$$s = \frac{4}{45}\pi^2 T^3 \left[1 + \frac{1}{288}\frac{T^4}{F^4}\left(8\ln\frac{T_p}{T} - 1 \right) + \mathcal{O}(T^6) \right],$$

$$c_V = \frac{4}{15}\pi^2 T^3 \left[1 + \frac{1}{864}\frac{T^4}{F^4}\left(56\ln\frac{T_p}{T} - 15 \right) + \mathcal{O}(T^6) \right]$$

$$(d=3+1,\ N=3). \tag{7.8}$$

These series, valid for the O(3) antiferromagnet in $d=3+1$, we now want to compare with the analogous series for $d=2+1$.

As we have seen, in three dimensions the parameter λ is finite and therefore no such scale, involving next-to-leading order coupling constants from $\mathcal{L}^4_{eff}$, arises in the low-temperature series of the thermodynamic quantities. In the limit $H \to 0$, the low-temperature expansions of the thermodynamic quantities for the O(3) antiferromagnet in $d=2+1$ take the form

$$P = \frac{\zeta(3)}{\pi}T^3 \left[1 - \frac{\pi q_1}{\zeta(3)}\frac{T^2}{F^4} + \mathcal{O}(T^3) \right],$$

$$u = \frac{2\zeta(3)}{\pi}T^3 \left[1 - \frac{2\pi q_1}{\zeta(3)}\frac{T^2}{F^4} + \mathcal{O}(T^3) \right],$$

$$s = \frac{3\zeta(3)}{\pi}T^2 \left[1 - \frac{5\pi q_1}{3\zeta(3)}\frac{T^2}{F^4} + \mathcal{O}(T^3) \right],$$

$$c_V = \frac{6\zeta(3)}{\pi}T^2 \left[1 - \frac{10\pi q_1}{3\zeta(3)}\frac{T^2}{F^4} + \mathcal{O}(T^3) \right] \quad (d=2+1,\ N=3). \tag{7.9}$$

Here we would expect the low-temperature series to proceed in steps of T since every loop in $d=2+1$ leads to an additional suppression of one power of the temperature. However, as it was the case for $d=3+1$, there are no next-to-leading order corrections in the above series for $d=2+1$: a term proportional to T^4 in the pressure is absent. Again, the corresponding two-loop graph 4b is proportional to M_π^2 [see Eq. (3.5)], such that it vanishes in the limit $H \to 0$, much like the constant a in $3+1$ dimensions before. In the absence of a staggered field, the magnon-magnon interaction both in $d=2+1$ and $d=3+1$ thus becomes very weak, as we are dealing with a next-to-next-to-leading order effect.

For nonzero external field, the low-temperature representations of the thermodynamic quantities retain their form, except that the coefficients now become functions of M_π/T. In the region $T \gg M_\pi$ one recovers the results of the theory for zero external field, whereas in the opposite limit, $T \ll M_\pi$, the gas is dilute and the particles move nonrelativistically. The properties of the system are therefore very sensitive to the value of the ratio M_π/T.

To illustrate this sensitivity, let us consider the pressure and discuss the general situation for $N>2$. In the limit $H \to 0$, as we have seen, a two-loop contribution of order p^6 in $d=3+1$—or p^4 in $d=2+1$—does not occur. This is no longer the case for an approximate symmetry ($H \neq 0$): remarkably, the sign of the corresponding interaction term of order p^6 ($\propto HT^4$, graph 6A) in $d=3+1$—or the corresponding interaction term of order p^4 ($\propto HT^2$, graph 4b) in $d=2+1$—turns out to be negative. With respect to the limit $H \to 0$, the sign of this interaction term is thus different: in the absence of an external field, the first nonleading term (order p^5 in $d=2+1$, order p^8 in $d=3+1$) is positive and the interaction among the Goldstone bosons thus repulsive. We conclude that a weak external field damps this repulsion among the Goldstone bosons, such that the effective interaction becomes even weaker.

Interestingly, the case $N=3$ is rather special: since the two-loop contribution both in $d=2+1$ and $d=3+1$ is proportional to $(N-3)$, the above-mentioned damping of the interaction does not occur. Still, the repulsive interaction between antiferromagnetic magnons in three or four dimensions is very weak as we are dealing with a next-to-next-to-leading order effect.

VIII. CONCLUSIONS

Condensed-matter systems exhibiting a spontaneously broken continuous symmetry may very efficiently be analyzed with the fully systematic method of effective Lagrangians. In the present study we have considered O(N) antiferromagnets in $d=2+1$ space-time dimensions which display a spontaneously broken internal rotation symmetry $O(N) \to O(N-1)$ and whose leading-order effective Lagrangian can be brought to (pseudo-)Lorentz-invariant form. The low-temperature properties of this system are dominated by the corresponding Goldstone bosons, which for $N=3$ may be identified with the two antiferromagnetic magnons or spin-wave excitations.

We have extended previous results for O(N) antiferromagnets in $d=2+1$ to higher orders in the derivative expansion, evaluating the partition function up to and including three-loop diagrams. Although the renormalization and the subsequent numerical evaluation of one particular three-loop graph turns out to be nontrivial, the calculation is perfectly feasible within the effective-field theory framework. One of our main results is that the interaction among magnons in the O(3)-invariant Heisenberg antiferromagnet, defined on a square or a honeycomb lattice, is very weak and repulsive at low temperatures, manifesting itself through a term proportional to five powers of the temperature in the pressure. Remarkably, the coefficient of this interaction term is fully determined by the leading-order effective Lagrangian $\mathcal{L}^2_{eff}$ and does not involve any higher-order effective constants from $\mathcal{L}^4_{eff}$—the symmetry is thus very restrictive in $d=2+1$. As we

have argued, additional effective constants in $\mathcal{L}^4_{eff}$, taking into account the Lorentz-noninvariant nature of the system, merely affect the renormalization of the magnon mass or yield higher-order corrections to the magnon dispersion law, but do not affect at all the leading contribution originating from the magnon-magnon interaction in the pressure.

The free energy density for O(N) antiferromagnets in $d=3+1$ up to the three-loop level, on the other hand, does involve coupling constants from $\mathcal{L}^4_{eff}$, which undergo logarithmic renormalization. Accordingly, the effective expansion of thermodynamic quantities now contains a scale related to these coupling constants in $\mathcal{L}^4_{eff}$. In four dimensions, within the (pseudo-)Lorentz-invariant framework, we thus need more phenomenological input, i.e., the numerical values of some next-to-leading order effective coupling constants, in order to fully specify the structure of the magnon-magnon interaction in the low-temperature series up to the three-loop level. Still, the symmetry is also very restrictive here, as it unambiguously fixes the coefficients in the expansion of the free energy density of O(N) antiferromagnets in $d=3+1$ up to order T^8, where the logarithm involving the scale enters.

The low-temperature theorems for the various thermodynamic quantities of O(N) antiferromagnets in three and four space-time dimensions are exact up to and including three loops: independently of the specific underlying model, they are valid for any system with a spontaneously broken symmetry $\mathrm{O}(N)\to\mathrm{O}(N-1)$, provided that the system can be described in a (pseudo-)Lorentz-invariant framework, with the velocity of light replaced by the spin-wave velocity. In particular, there are no approximations or idealizations involved in our main result regarding the weakness and the repulsive character of the magnon-magnon interaction in the O(3) antiferromagnet in $d=2+1$: although we use a (pseudo-)Lorentz-invariant framework, our calculation is not just some kind of "academic" exercise, as the lattice anisotropies, or the Lorentz-noninvariant nature of the system in general, cannot manifest themselves in the magnon-magnon interaction up to the three-loop order of the perturbative expansion, considered in the present paper—hence our calculation applies, as it stands, to the quantum Heisenberg antiferromagnet defined on a square or a honeycomb lattice.

We would like to emphasize that the order of the calculation presented here, as we have argued in Sec. V, appears to be beyond the reach of any realistic microscopic calculation based on spin-wave theory or other standard condensed-matter methods, such as Schwinger boson mean-field theory. The fully systematic effective Lagrangian method thus clearly proves to be more efficient than the complicated microscopic analysis. Another virtue of the effective Lagrangian technique is that it addresses the problem from a unified and model-independent point of view based on symmetry—at large wavelengths, the microscopic structure of the system only manifests itself in the numerical values of a few coupling constants. Therefore the effective Lagrangian method is ideally suited to understand similarities and differences in the structure of the low-temperature series for antiferromagnets in three and four dimensions based on symmetry considerations only.

ACKNOWLEDGMENTS

The author would like to thank H. Leutwyler and U.-J. Wiese for stimulating discussions and for useful comments regarding the manuscript. This work was supported by CONACYT through Grant No. 50744-F.

APPENDIX A: EVALUATION OF THE CATEYE GRAPH IN $d=2+1$

The singularities contained in the integrals J_1 and J_2, originating from the cateye graph 5c, may be removed by subtracting suitable counterterms. Since our main focus is the O(3) antiferromagnet, here we only discuss the renormalization of the function J_2—the renormalization of the quantity J_1, which does not contribute to the free energy density for $N=3$ according to Eq. (3.14), will be discussed elsewhere.

The singularities contained in J_2 may be removed by subtracting the following counterterms,

$$\bar{J}_2 = J_2 - c_3 - c_4 g_1(M,T). \tag{A.1}$$

To establish this result, we use a method, developed in Ref. 22, which at the same time also provides us with a representation of the renormalized integrals suitable for numerical evaluation. We first cut out a sphere $\mathcal{S}$ around the origin of radius $|\mathcal{S}|\leq\beta/2$ and decompose J_2 accordingly,

$$J_2 = \int_{\mathcal{S}} d^dx\{\partial_\mu G(x)\partial_\mu G(x)\}^2 + \int_{\mathcal{T}\backslash\mathcal{S}} d^dx\{\partial_\mu G(x)\partial_\mu G(x)\}^2. \tag{A.2}$$

In the integral over the complement $\mathcal{T}\backslash\mathcal{S}$ of the sphere, the integrand is not singular and the limit $d\to 3$ can readily be taken. In the integral over the sphere, we insert the decomposition, Eq. (4.1),

$$\begin{aligned} J_2 = \int_{\mathcal{S}} d^dx(\{\partial_\mu\bar{G}\partial_\mu\bar{G}\}^2 &+ 4\partial_\mu\bar{G}\partial_\mu\bar{G}\partial_\nu\bar{G}\partial_\nu\Delta \\ &+ 4\partial_\mu\bar{G}\partial_\mu\Delta\partial_\nu\bar{G}\partial_\nu\Delta + 2\partial_\mu\bar{G}\partial_\mu\bar{G}\partial_\nu\Delta\partial_\nu\Delta \\ &+ 4\partial_\mu\bar{G}\partial_\mu\Delta\partial_\nu\Delta\partial_\nu\Delta + \{\partial_\mu\Delta\partial_\mu\Delta\}^2). \end{aligned} \tag{A.3}$$

In $d=2+1$ the first four terms are convergent. However, the last two terms, involving three and four nonthermal propagators, respectively, are divergent.

In order to extract these two singularities showing up in $d=2+1$, we follow Ref. 22, where the dimension was $d=3+1$. We first disregard derivatives and consider the expression $4\bar{G}\Delta^3$, which contains three nonthermal propagators. Since $\Delta(x)$ is Euclidean invariant, the integral

$$\int_{\mathcal{S}} d^dx 4\bar{G}\Delta^3 \tag{A.4}$$

only involves the angular average of $\bar{G}(x)$,

$$f(R) = \int d^{d-1}\Omega\bar{G}(x), \quad R=|x|. \tag{A.5}$$

The differential equation

$$\Box \bar{G} = M^2 \bar{G} \tag{A.6}$$

implies

$$\left(\frac{d^2}{dR^2} + \frac{d-1}{R} \frac{d}{dR} - M^2 \right) f = 0, \quad R < \beta. \tag{A.7}$$

Since f is regular at the origin, the differential equation fixes it uniquely up to a constant. The function $g_1\, ch(Mx_4)$ obeys the same differential equation as $\bar{G}(x)$ and coincides with it at the origin. The angular averages of these two quantities are therefore the same, i.e.,

$$\int_{\mathcal{S}} d^d x \bar{G} \Delta^3 = g_1 \int_{\mathcal{S}} d^d x ch(Mx_4) \Delta^3. \tag{A.8}$$

We split the integral over the sphere into two pieces,

$$4g_1 \int_{\mathcal{S}} d^d x ch(Mx_4) \Delta^3 = 4g_1 \int_{\mathcal{R}} d^d x ch(Mx_4) \Delta^3 - 4g_1 \int_{\mathcal{R}\setminus\mathcal{S}} d^d x ch(Mx_4) \Delta^3, \tag{A.9}$$

where the singularity is now contained in the integral over all Euclidean space in the form of the counterterm

$$c_2 = 4 \int_{\mathcal{R}} d^d x ch(Mx_4) \Delta^3. \tag{A.10}$$

The same line of reasoning goes through for the expression $4\partial_\mu \bar{G} \partial_\mu \Delta \partial_\nu \Delta \partial_\nu \Delta$ in Eq. (A.3), where one ends up with the counterterm

$$c_4 = 4 \int_{\mathcal{R}} d^d x \partial_\mu ch(Mx_4) \partial_\mu \Delta \partial_\nu \Delta \partial_\nu \Delta. \tag{A.11}$$

As far as the last term in Eq. (A.3), involving four nonthermal propagators, is concerned, it suffices to subtract the temperature-independent integral of $\{\partial_\mu \Delta(x) \partial_\mu \Delta(x)\}^2$ over all Euclidean space,

$$c_3 = \int_{\mathcal{R}} d^d x \{\partial_\mu \Delta \partial_\mu \Delta\}^2, \tag{A.12}$$

in order to remove the singularity. Collecting the various pieces, we thus arrive at the following representation for the renormalized integral in $d=2+1$,

$$\bar{J}_2 = \int_{\mathcal{T}} d^3 x T + \int_{\mathcal{T}\mathcal{S}} d^3 x U - \int_{\mathcal{R}\setminus\mathcal{S}} d^3 x \partial_\mu \Delta \partial_\mu \Delta \cdot W,$$

$$T = (\partial_\mu \bar{G} \partial_\mu \bar{G})^2 + 4\partial_\mu \bar{G} \partial_\mu \bar{G} \partial_\nu \bar{G} \partial_\nu \Delta + 4\partial_\mu \bar{G} \partial_\mu \Delta \partial_\nu \bar{G} \partial_\nu \Delta + 2\partial_\mu \bar{G} \partial_\mu \bar{G} \partial_\nu \Delta \partial_\nu \Delta,$$

$$U = 4\partial_\mu \bar{G} \partial_\mu \Delta \partial_\nu \Delta \partial_\nu \Delta + \partial_\mu \Delta \partial_\mu \Delta \partial_\nu \Delta \partial_\nu \Delta,$$

$$W = 4g_1 \partial_\mu ch(Mx_4) \partial_\mu \Delta + \partial_\mu \Delta \partial_\mu \Delta. \tag{A.13}$$

This expression involves ordinary, convergent integrals. Exploiting the fact that $\bar{G}(x)$ and $\Delta(x)$ only depend on $r=|\vec{x}|$ and on $t=x_4$, the integrals occurring in this representation become effectively two dimensional,

$$d^3 x = 2\pi r dr dt. \tag{A.14}$$

Note that the quantity $\bar{J}_2$ must be independent of the size of the sphere—this provides us with a welcome numerical consistency check of our calculation.

It is instructive to compare our decomposition of the integrals, Eq. (A.13), with the decomposition originally used in Ref. 22, which in $d=2+1$ amounts to

$$\bar{J}_2 = \int_{\mathcal{T}\mathcal{S}} d^3 x \tilde{U} + \int_{\mathcal{S}} d^3 x \tilde{V} - \int_{\mathcal{R}\setminus\mathcal{S}} d^3 x \partial_\mu \Delta \partial_\mu \Delta \cdot \tilde{W},$$

$$\tilde{U} = (\partial_\mu G \partial_\mu G)^2,$$

$$\tilde{V} = (\partial_\mu \bar{G} \partial_\mu \bar{G})^2 + 4\partial_\mu \bar{G} \partial_\mu \bar{G} \partial_\nu \bar{G} \partial_\nu \Delta + 2Q_{\mu\mu} \partial_\nu \Delta \partial_\nu \Delta + 4Q_{\mu\nu} \partial_\mu \Delta \partial_\nu \Delta,$$

$$\tilde{W} = \tilde{w} + 4g_1 \partial_\mu ch(Mx_4) \partial_\mu \Delta + \partial_\mu \Delta \partial_\mu \Delta \tag{A.15}$$

with

$$\tilde{w} = \frac{1}{x^2} \left[\left(\frac{3}{2} x^4 - \frac{9}{2} x^2 x_4^2 + 9x_4^4 \right) g_0^2 + 12M^2 x_4^4 g_0 g_1 + 2(2M^4 x_4^4 + M^4 x^2 x_4^2) g_1^2 \right],$$

$$Q_{\mu\nu} = \partial_\mu \bar{G}(x) \partial_\nu \bar{G}(x) - \bar{G}_{\mu\alpha} \bar{G}_{\nu\beta} x_\alpha x_\beta,$$

$$\bar{G}_{\mu\nu} = -\frac{1}{2} \delta_{\mu\nu} g_0 + \delta_\mu^4 \delta_\nu^4 \left(\frac{3}{2} g_0 + M^2 g_1 \right). \tag{A.16}$$

The main difference between the two decompositions, Eqs. (A.13) and (A.15), concerns the terms involving two thermal propagators, where we have

$$\int_{\mathcal{S}} d^3 x (2\partial_\mu \bar{G} \partial_\mu \bar{G} \partial_\nu \Delta \partial_\nu \Delta + 4\partial_\mu \bar{G} \partial_\mu \Delta \partial_\nu \bar{G} \partial_\nu \Delta)$$

$$= \int_{\mathcal{S}} d^3 x (2Q_{\mu\mu} \partial_\nu \Delta \partial_\nu \Delta + 4Q_{\mu\nu} \partial_\mu \Delta \partial_\nu \Delta) - \int_{\mathcal{R}\setminus\mathcal{S}} d^3 x \partial_\mu \Delta \partial_\mu \Delta \cdot \tilde{w} + \int_{\mathcal{R}} d^3 x (2\bar{G}_{\mu\alpha} \bar{G}_{\mu\beta} x_\alpha x_\beta \partial_\nu \Delta \partial_\nu \Delta + 4\bar{G}_{\mu\alpha} \bar{G}_{\nu\beta} x_\alpha x_\beta \partial_\mu \Delta \partial_\nu \Delta). \tag{A.17}$$

Now, in four dimensions the integral over the sphere on the left-hand side contains a logarithmic singularity—this was the reason why in Ref. 22 the above decomposition was performed: the singularity then occurs again on the right-hand side in the integral over all Euclidean space. It turns out that,

in order to renormalize the integral J_2 in $d=3+1$, it is thus not sufficient to just subtract the two counterterms c_3 and c_4 in Eq. (A.1)—rather, one has to subtract two more terms,

$$\bar{J}_2 = J_2 - c_3 - c_4 g_1 + \frac{1}{3}(d+6)(d-2)\lambda(\bar{G}_{\mu\nu})^2 + \frac{2}{3}(d-2)\lambda M^4 (g_1)^2, \tag{A.18}$$

in order to remove all singularities in J_2.

In three dimensions, as we have seen, the integral over the sphere on the left-hand side of Eq. (A.17) is not singular. Likewise the integral over all Euclidean space on the right-hand side is perfectly well defined, such that there is no need to introduce the above decomposition, Eq. (A.15), in three dimensions in the first place. Still, in order to check that our entire calculation is consistent, we have verified both analytically and numerically that the evaluation of the quantity $\bar{J}_2$ via Eqs. (A.13) and (A.15) yields the same result.

We close this section with a comment regarding dimensional regularization and the different structure of the singularities in three and four dimensions, respectively. The essential point can be seen in the identity, Eq. (A.17), which involves two thermal propagators. In four dimensions, as we have seen, the cateye graph is of order p^8 and so is the singularity occurring in the last term of Eq. (A.17). Now, in four dimensions we also have two-loop graphs which are of the same order p^8: graphs 8D and 8E (see Fig. 2) which involve vertices from the next-to-leading order effective Lagrangian $\mathcal{L}^4_{eff}$. Therefore, the singularities in the last term of Eq. (A.17)—the integral over all Euclidean space—can be absorbed into a combination of these next-to-leading order coupling constants.

In three dimensions, on the other hand, these two-loop graphs are of order p^6, i.e., beyond the order p^5 considered in the present work. Loosely speaking, there is no communication between the cateye graph (order p^5) and these two-loop graphs of order p^6 and it so seems that—in three dimensions—the "singularities" in the last term of Eq. (A.17) cannot be absorbed, as there are no next-to-leading order coupling constants available. However, in three dimensions the parameter λ arising in the last term of Eq. (A.17) is finite, such that the bookkeeping of "divergences" in three dimensions is perfectly consistent.

APPENDIX B: RENORMALIZATION

In this appendix, we would like to derive expression (4.9) for the free energy density of an O(N) antiferromagnet in $d=2+1$. We first show that all the terms in the free energy density, Eq. (3.14), that are linear in the kinematical functions $g_r(M,T)$ can be merged into a single such function, namely, g_0, by replacing the bare mass M with the physical mass M_π.

With the decompositions, Eqs. (4.2) and (4.5), the terms in the free energy density, Eq. (3.14), linear in $g_r(M,T)$ read

$$\begin{aligned} z^{\{1\}} = &-\frac{1}{2}(N-1)g_0(M,T) + \frac{1}{2}(N-1)(N-3)\frac{M^4}{F^2}\lambda g_1(M,T) \\ &- \frac{1}{4}(N-1)(N-3)^2\frac{M^8}{F^4}\lambda^2 g_2(M,T) + (N-1)(k_2 \\ &- k_1)\frac{M^4}{F^2}g_1(M,T) + \frac{1}{48}c_2(N-1)(N-3)\frac{M^4}{F^4}g_1(M,T) \\ &- \frac{1}{4}c_4(N-1)(N-2)\frac{1}{F^4}g_1(M,T) \\ &+ \frac{1}{2}(N-1)(N-3)(2N-5)\frac{M^6}{F^4}\lambda^2 g_1(M,T). \end{aligned} \tag{B.1}$$

Now the pressure at low temperatures is of order $\exp(-M_\pi/T)$ originating from one-particle states—states containing two or more Goldstone bosons only show up at order $\exp(-2M_\pi/T)$. Therefore it is possible to extract the physical Goldstone boson mass M_π from the behavior of the pressure at low temperatures,

$$M_\pi = -\lim_{T\to 0} T \ln P. \tag{B.2}$$

Using the relation

$$g_{r+1} = -\frac{dg_r}{dM^2}, \tag{B.3}$$

this limit amounts to

$$M_\pi^2 = M^2 + (N-3)\lambda\frac{M^4}{F^2} + \left\{2(k_2-k_1) + \frac{b_1}{F^2} + \frac{b_2\lambda^2 M^2}{F^2}\right\}\frac{M^4}{F^2} + \mathcal{O}(M^5), \tag{B.4}$$

where the coefficients b_1 and b_2 are given by

$$b_1 = \frac{1}{24}(N-3)\gamma_2 - \frac{1}{2}(N-2)\gamma_4,$$

$$b_2 = (N-3)(2N-5). \tag{B.5}$$

The quantities γ_2 and γ_4 are singular functions of the dimension d and are related to the coefficients c_2 and c_4—defined in Eqs. (A.10) and (A.11)—as follows:

$$c_2 = \gamma_2 M^{2d-6}, \quad c_4 = \gamma_4 M^{2d-2}. \tag{B.6}$$

Inspecting the curly bracket in formula (B.4) one thus notices that the infinities contained in c_2 and c_4, which stem from the three-loop graph 5c, are absorbed into the combination k_2-k_1 of next-to-leading order coupling constants, originating from the one-loop graph 5d. Note that in $d=2+1$ the parameter λ is finite, such that second term on the right-hand side of Eq. (B.4), coming from the two-loop graph 4b, does not contain any singularities.

One readily verifies that the replacement $g_0(M,T) \to g_0(M_\pi,T)$ in the first term of Eq. (B.1) cancels all other terms linear in $g_r(M,T)$. The free energy density, linear in the kinematical functions, thus takes the simple form

$$-\frac{1}{2}(N-1)g_0(M_\pi,T). \tag{B.7}$$

We now proceed with the terms in the free energy density that are quadratic in the kinematical functions $g_r(M,T)$. They are

$$z^{\{2\}} = \frac{1}{8}(N-1)(N-3)\frac{M^2}{F^2}g_1(M,T)^2 + \frac{1}{16}(N-1)(N-3)(7N-17)\frac{M^4}{F^4}\lambda g_1(M,T)^2 - \frac{1}{4}(N-1)(N-3)^2\frac{M^6}{F^4}\lambda g_1(M,T)g_2(M,T). \tag{B.8}$$

In the first term we make the replacement $g_1(M,T)\to g_1(M_\pi,T)$, which amounts to

$$g_1(M_\pi,T)^2 = g_1(M,T)^2 - \left\{2(N-3)\frac{M^4}{F^2}\lambda + \mathcal{O}(M^4)\right\} \times g_1(M,T)g_2(M,T). \tag{B.9}$$

One notices that this cancels the third term in Eq. (B.8). We are thus left with

$$\frac{1}{8}(N-1)(N-3)\frac{M^2}{F^2}g_1(M_\pi,T)^2 + \frac{1}{16}(N-1)(N-3)(7N-17)\frac{M_\pi^4}{F^4}\lambda g_1(M_\pi,T)^2. \tag{B.10}$$

Note that in the second term we have also replaced the bare mass by the physical mass, both in the prefactor and in the kinematical function: this is legitimate as the difference is beyond our accuracy. Finally, in the prefactor of the first term, we also express the bare mass by the physical mass using relation (B.4), obtaining the following terms in the free energy density quadratic in the kinematical functions,

$$\frac{1}{8}(N-1)(N-3)\frac{M_\pi^2}{F^2}g_1(M_\pi,T)^2 + \frac{1}{16}(N-1)(N-3)(5N-11)\frac{M_\pi^4}{F^4}\lambda g_1(M_\pi,T)^2. \tag{B.11}$$

To end up, we take care of the remaining terms in the free energy density that are either cubic in the kinematical functions $g_r(M,T)$ or are related to integrals over the torus,

$$z^{\{3\}} = \frac{1}{48}(N-1)(N-3)(3N-7)\frac{M^2}{F^4}g_1(M,T)^3 - \frac{1}{16}(N-1)(N-3)^2\frac{M^4}{F^4}g_1(M,T)^2g_2(M,T) + \frac{1}{48}(N-1)(N-3)\frac{M^4}{F^4}\bar{J}_1 - \frac{1}{4}(N-1)(N-2)\frac{1}{F^4}\bar{J}_2. \tag{B.12}$$

Again, we replace the bare mass by the physical mass in the above terms, both in the kinematical functions and in the prefactors, as the difference is beyond our accuracy. No cancellations of terms occur here.

Collecting the various contributions, we arrive at the expression for the free energy density of an O(N) antiferromagnet in $d=2+1$,

$$z = z_0 - \frac{1}{2}(N-1)g_0 + \frac{1}{8}(N-1)(N-3)\frac{M_\pi^2}{F^2}(g_1)^2 - \frac{1}{128\pi}(N-1)(N-3)(5N-11)\frac{M_\pi^3}{F^4}(g_1)^2 + \frac{1}{48}(N-1)(N-3)(3N-7)\frac{M_\pi^2}{F^4}(g_1)^3 - \frac{1}{16}(N-1)(N-3)^2\frac{M_\pi^4}{F^4}(g_1)^2g_2 + \frac{1}{48}(N-1)(N-3)\frac{M_\pi^4}{F^4}\bar{J}_1 - \frac{1}{4}(N-1)(N-2)\frac{1}{F^4}\bar{J}_2 + \mathcal{O}(p^6). \tag{B.13}$$

Note that only the physical mass M_π occurs in the above formula: in particular, the kinematical functions are $g_r=g_r(M_\pi,T)$. Remember that the temperature-independent contribution z_0 is the vacuum energy density given in Eq. (4.6).

APPENDIX C: PROPERTIES OF THE KINEMATICAL FUNCTIONS $g_r(M,T)$

In this appendix we discuss some properties of the kinematical functions $g_r(M,T)$, defined by

$$g_r(M,T) = 2\int_0^\infty \frac{d\rho}{(4\pi\rho)^{d/2}}\rho^{r-1}\exp(-\rho M^2) \times \sum_{n=1}^{\infty}\exp(-n^2/4\rho T^2). \tag{C.1}$$

We follow the appendices A and B of Ref. 1 where the analogous kinematical functions for finite volume were considered. Here we adapt the method described therein to finite temperature.

We are particularly interested in the expansion of $g_r(M,T)$ in the limit $M\to 0$, where infrared singularities occur. We introduce the Jacobi theta function,

$$S(x) = \sum_{n=-\infty}^{\infty} e^{-\pi n^2 x}, \tag{C.2}$$

and express the kinematical function (C.1) by

$$g_r(M,T) = \frac{T^{d-2r}}{(4\pi)^r}\int_0^\infty dt t^{r-d/2-1}\exp\left(-\frac{M^2t}{4\pi T^2}\right)\times[S(1/t)-1]. \tag{C.3}$$

The integration is split into two regions, $0\le t\le 1$ and $1\le t<\infty$. In the second region we use the identity

$$S(x) = \frac{1}{\sqrt{x}} S(1/x), \tag{C.4}$$

change the integration variable $t \to 1/t$, and arrive at the following representation for the kinematical functions $g_r(M,T)$,

$$g_r(M,T) = \frac{T^{d-2r}}{(4\pi)^r}\{\tilde{a}_r + b_{r-d/2+1/2} - b_{r-d/2}\}, \tag{C.5}$$

with

$$\tilde{a}_r = \int_0^1 dt t^{r-d/2-1} \exp\left(-\frac{M^2 t}{4\pi T^2}\right)[S(1/t)-1] + \int_0^1 dt t^{-r+d/2-3/2} \exp\left(-\frac{M^2}{4\pi T^2 t}\right)[S(1/t)-1] \tag{C.6}$$

and

$$b_s = \int_1^\infty dt t^{s-1} \exp\left(-\frac{M^2 t}{4\pi T^2}\right). \tag{C.7}$$

The function $\tilde{a}_r$ does not contain infrared singularities and the expansion in powers of M^2 is of the form

$$\tilde{a}_r = \sum_{n=0}^\infty \left(-\frac{M^2}{4\pi T^2}\right)^n \frac{1}{n!}\{\hat{\alpha}_{r+n-d/2} + \hat{\alpha}_{-r-n+d/2-1/2}\}, \tag{C.8}$$

where

$$\hat{\alpha}_p = \int_0^1 dt t^{p-1}\{S(1/t)-1\}. \tag{C.9}$$

The infrared singularities are contained in the incomplete Γ function b_s,

$$b_s = \left(\frac{M^2}{4\pi T^2}\right)^{-s}\Gamma(s) - \sum_{n=0}^\infty \frac{1}{n!}\left(-\frac{M^2}{4\pi T^2}\right)^n \frac{1}{n+s}. \tag{C.10}$$

The pole in the function $\Gamma(s)$ at $s=0,-1,-2,\ldots$ is compensated by a pole occurring in the second piece of b_s which is analytic in M. The two singularities can be merged and one ends up with a logarithmic contribution. Details can be found in Ref. 1—here we give the explicit expression for $b_{-N}(N \geq 0)$,

$$b_{-N} = \frac{(-1)^{N+1}}{N!}\left(\frac{M^2}{4\pi T^2}\right)^N \left\{\log\frac{M^2}{4\pi T^2} + \gamma - \sum_{n=1}^N \frac{1}{n}\right\} + \sum_{n\neq N} \frac{1}{n!}\left(-\frac{M^2}{4\pi T^2}\right)^n \frac{1}{N-n}, \tag{C.11}$$

where the quantity $\gamma \approx 0.577$ denotes Euler's constant. Note that, in the second sum over n, the value $n=N$ is to be omitted. Moreover, for $N=0$ the sum in the curly bracket is to be omitted.

We now consider the kinematical function $g_0(M,T)$ both in three and four dimensions. According to Eq. (C.5) we have

$$g_0^{d=3}(M,T) = T^3\{\tilde{a}_0 + b_{-1} - b_{-3/2}\},$$
$$g_0^{d=4}(M,T) = T^4\{\tilde{a}_0 + b_{-3/2} - b_{-2}\}. \tag{C.12}$$

Using relation (C.4) and the identity

$$\pi^{-z/2}\Gamma(z/2)\zeta(z) = \frac{1}{2}\int_0^\infty dt t^{z/2-1}\{S(t)-1\}, \tag{C.13}$$

one readily shows that the various contributions in Eq. (C.12) can be merged into a single series in M, involving Riemann zeta functions,

$$g_0^{d=3}(M,T) = T^3\left[\frac{\zeta(3)}{\pi} + \frac{1}{4\pi}\frac{M^2}{T^2}\left\{\ln\frac{M^2}{T^2} - 1\right\} - \frac{1}{6\pi}\frac{M^3}{T^3} + 2\pi\sum_{n=2}^\infty \frac{(-1)^n}{n!}\left(\frac{M}{2\pi T}\right)^{2n}\Gamma(n-1)\zeta(2n-2)\right],$$

$$g_0^{d=4}(M,T) = T^4\left[\frac{\pi^2}{45} - \frac{1}{12}\frac{M^2}{T^2} + \frac{1}{6\pi}\frac{M^3}{T^3} + \frac{\left(2\gamma - \frac{3}{2}\right)}{32\pi^2}\frac{M^4}{T^4} + \frac{1}{32\pi^2}\frac{M^4}{T^4}\ln\frac{M^2}{16\pi^2 T^2} + 2\pi^{3/2}\sum_{n=3}^\infty \frac{(-1)^n}{n!} \times \left(\frac{M}{2\pi T}\right)^{2n}\Gamma\left(n-\frac{3}{2}\right)\zeta(2n-3)\right] \quad (T \gg M). \tag{C.14}$$

Explicitly, the first few terms in these series read

$$g_0^{d=3}(M,T) = \frac{1}{\pi}T^3\left[\zeta(3) - \frac{1}{4}\frac{M^2}{T^2} + \frac{1}{4}\frac{M^2}{T^2}\ln\frac{M^2}{T^2} - \frac{1}{6}\frac{M^3}{T^3} + \frac{1}{96}\frac{M^4}{T^4} + \mathcal{O}\left(\frac{M}{T}\right)^6\right],$$

$$g_0^{d=4}(M,T) = \frac{\pi^2}{45}T^4\left[1 - \frac{15}{4\pi^2}\frac{M^2}{T^2} + \frac{15}{2\pi^3}\frac{M^3}{T^3} + \frac{45\left(\gamma - \frac{3}{4} - \ln 4\pi\right)}{16\pi^4}\frac{M^4}{T^4} + \frac{45}{32\pi^4}\frac{M^4}{T^4}\ln\frac{M^2}{T^2} + \mathcal{O}\left(\frac{M}{T}\right)^6\right] \quad (T \gg M). \tag{C.15}$$

The expansion for the function $g_0^{d=4}(M,T)$ coincides with the expression derived in the appendix of Ref. 22, where a different method was used. The series for the kinematical functions $g_1(M,T)$ and $g_2(M,T)$ can readily be obtained using the relation

$$g_{r+1} = -\frac{dg_r}{dM^2}. \tag{C.16}$$

[1] P. Hasenfratz and H. Leutwyler, Nucl. Phys. B **343**, 241 (1990).
[2] H. Leutwyler, Phys. Rev. D **49**, 3033 (1994).
[3] C. P. Hofmann, Phys. Rev. B **60**, 388 (1999).
[4] C. P. Hofmann, Phys. Rev. B **60**, 406 (1999).
[5] S. Chakravarty, B. I. Halperin, and D. R. Nelson, Phys. Rev. B **39**, 2344 (1989).
[6] H. Neuberger and T. Ziman, Phys. Rev. B **39**, 2608 (1989).
[7] D. S. Fisher, Phys. Rev. B **39**, 11783 (1989).
[8] P. Hasenfratz and F. Niedermayer, Z. Phys. B: Condens. Matter **92**, 91 (1993).
[9] B. Borasoy, in *The Standard Model and Beyond*, edited by T. Aliev, N. K. Pak, and M. Serin (Springer, Berlin, 2008), p. 1; C. P. Burgess, Annu. Rev. Nucl. Part. Sci. **57**, 329 (2007); V. Bernard and U.-G. Meissner, *ibid.* **57**, 33 (2007); B. Kubis, arXiv:hep-ph/0703274 (unpublished); S. Scherer and M. R. Schindler, arXiv:hep-ph/0505265 (unpublished); J. L. Goity, Czech. J. Phys. **51**, B35 (2001); S. Scherer, Adv. Nucl. Phys. **27**, 277 (2003); B. R. Holstein, arXiv:hep-ph/0010033 (unpublished); arXiv:hep-ph/9510344 (unpublished); A. Pich, arXiv:hep-ph/9806303 (unpublished); V. Koch, Int. J. Mod. Phys. E **6**, 203 (1997); G. Ecker, arXiv:hep-ph/9608226 (unpublished); Prog. Part. Nucl. Phys. **35**, 1 (1995); A. V. Manohar, in *Perturbative and Nonperturbative Aspects of Quantum Field Theory*, edited by H. Latal and W. Schweiger (Springer, New York, 1997), p. 311.
[10] B. Moussallam, arXiv:hep-ph/0407246 (unpublished); G. Colangelo and G. Isidori, arXiv:hep-ph/0101264 (unpublished); J. Gasser, Nucl. Phys. B, Proc. Suppl. **86**, 257 (2000); C. P. Burgess, Fourth International Symposium on Radiative Corrections (RADCOR 98): Application of Quantum Field Theory to Phenomenology, Barcelona, 1998 (unpublished), p. 471; arXiv:hep-ph/9812468 (unpublished); H. Leutwyler, arXiv:hep-ph/9409422 (unpublished).
[11] C. P. Hofmann, Phys. Rev. B **65**, 094430 (2002).
[12] J. M. Román and J. Soto, Int. J. Mod. Phys. B **13**, 755 (1999); Phys. Rev. B **62**, 3300 (2000); Ann. Phys. (N.Y.) **273**, 37 (1999).
[13] C. P. Burgess, Phys. Rep. **330**, 193 (2000); C. P. Burgess and C. A. Lutken, Phys. Rev. B **57**, 8642 (1998).
[14] F. Kämpfer, M. Moser, and U.-J. Wiese, Nucl. Phys. B **729**, 317 (2005); C. Brügger, F. Kämpfer, M. Moser, M. Pepe, and U.-J. Wiese, Phys. Rev. B **74**, 224432 (2006).
[15] U. Gerber, C. P. Hofmann, F.-J. Jiang, M. Nyfeler, and U.-J. Wiese, J. Stat. Mech.: Theory Exp. 2009, P03021.
[16] C. Brügger, F. Kämpfer, M. Pepe, and U.-J. Wiese, Eur. Phys. J. B **53**, 433 (2006); C. Brügger, C. P. Hofmann, F. Kämpfer, M. Pepe, and U.-J. Wiese, Phys. Rev. B **75**, 014421 (2007); C. Brügger, C. P. Hofmann, F. Kämpfer, M. Moser, M. Pepe, and U.-J. Wiese, *ibid.* **75**, 214405 (2007); F.-J. Jiang, F. Kämpfer, C. P. Hofmann, and U.-J. Wiese, Eur. Phys. J. B **69**, 473 (2009).
[17] H. Leutwyler, Ann. Phys. (N.Y.) **235**, 165 (1994).
[18] S. Weinberg, Physica A **96**, 327 (1979).
[19] Note also, that this counting scheme only applies within a Lorentz-invariant framework: loop corrections involving ferromagnetic magnons, e.g., which follow a quadratic dispersion relation, are suppressed by three powers of momentum in four space-time dimensions and suppressed by two powers of momentum in three space-time dimensions.
[20] H. Leutwyler, Nucl. Phys. B, Proc. Suppl. **4**, 248 (1988); in *New Theories in Physics*, Warsaw International Symposium on Elementary Particle Physics, Kazimierz, 1988, edited by Z. Ajduk, S. Pokorski, and A. Trautman (World Scientific, Singapore, 1989), p. 116; also in *Symmetry Violations in Subatomic Physics*, Summer Institute in Theoretical Physics, Kingston, 1988, edited by B. Castel and P. J. O'Donnell (World Scientific, Singapore, 1989), p. 57.
[21] N. P. Landsman and C. G. van Weert, Phys. Rep. **145**, 141 (1987); J. I. Kapusta, *Finite-Temperature Field Theory* (Cambridge University Press, Cambridge, England, 1989); A. V. Smilga, Phys. Rep. **291**, 1 (1997); J. Zinn-Justin, arXiv:hep-ph/0005272 (unpublished).
[22] P. Gerber and H. Leutwyler, Nucl. Phys. B **321**, 387 (1989).
[23] D. P. Arovas and A. Auerbach, Phys. Rev. B **38**, 316 (1988); **40**, 791 (1989); A. Auerbach and D. P. Arovas, Phys. Rev. Lett. **61**, 617 (1988).
[24] Y. Okabe, M. Kikuchi, and A. D. S. Nagi, Phys. Rev. Lett. **61**, 2971 (1988).
[25] T. Barnes, Int. J. Mod. Phys. C **2**, 659 (1991).
[26] N. D. Mermin and H. Wagner, Phys. Rev. Lett. **17**, 1133 (1966).
[27] P. Hasenfratz and F. Niedermayer, Phys. Lett. B **245**, 529 (1990).
[28] U.-J. Wiese and H. P. Ying, Z. Phys. B: Condens. Matter **93**, 147 (1994); B. B. Beard, R. J. Birgeneau, M. Greven, and U.-J. Wiese, Phys. Rev. Lett. **80**, 1742 (1998).
[29] J. Gasser and H. Leutwyler, Phys. Lett. B **184**, 83 (1987); **188**, 477 (1987); Nucl. Phys. B **307**, 763 (1988).
[30] H. Leutwyler, Phys. Lett. B **189**, 197 (1987).
[31] M. Göckeler and H. Leutwyler, Phys. Lett. B **253**, 193 (1991); Nucl. Phys. B **350**, 228 (1991).
[32] I. Dimitrovic, J. Nager, K. Jansen, and T. Neuhaus, Phys. Lett. B **268**, 408 (1991).
[33] See Sec. 4 of Ref. 8.